N2 modified dinucleotide cap analogs as a potent tool for mRNA engineering

RENATA GRZELA,[1] KAROLINA PIECYK,[2] ANNA STANKIEWICZ-DROGON,[1] PAULINA PIETROW,[2] MACIEJ LUKASZEWICZ,[1] KAROL KURPIEJEWSKI,[2] EDWARD DARZYNKIEWICZ,[1,3] and MARZENA JANKOWSKA-ANYSZKA[2]

[1]Division of Biophysics, Institute of Experimental Physics, University of Warsaw, 02-093 Warsaw, Poland
[2]Faculty of Chemistry, University of Warsaw, 02-093 Warsaw, Poland
[3]Center of New Technologies, University of Warsaw, 02-097 Warsaw, Poland

ABSTRACT

mRNA-based vaccines are relatively new technologies that have been in the field of interest of research centers and pharmaceutical companies in recent years. Such therapeutics are an attractive alternative for DNA-based vaccines since they provide material that can be used with no risk of genomic integration. Additionally, mRNA can be quite easily engineered to introduce modifications for different applications or to modulate its properties, for example, to increase translational efficiency or stability, which is not available for DNA vectors. Here, we describe the use of N2 modified dinucleotide cap analogs as components of mRNA transcripts. The compounds obtained showed very promising biological properties while incorporated into mRNA. The presented N2-guanine modifications within the cap structure ensure proper attachment of the dinucleotide to the transcripts in the IVT reaction, guarantees their incorporation only in the correct orientation, and enables highly efficient translation of mRNA both in the in vitro translation system and in human HEK293 cells.

Keywords: cap analogs; mRNA; cap-dependent translation; mRNA therapeutics; mRNA technology

INTRODUCTION

For over 20 years, mRNA-based technologies have been an area of intense investigation of research centers and pharmaceutical companies. As a result, at the outbreak of the COVID-19 pandemic, mRNA vaccines could be developed that became "the frontrunners" in the fight against this serious threat to the health and life of people all over the world (Polack et al. 2020; Baden et al. 2021). Earlier, the most widely studied nucleic acid-based vaccines were those encoded in DNA vectors. DNA-based vaccines, however, have some serious drawbacks: not only do they pose a risk for severe toxicity at high doses, but they can also integrate into the host genome, which in turn can lead to the activation of oncogenes (Raper et al. 2003). In contrast, mRNA-based vaccines provide an attractive alternative since they do not present the disadvantages mentioned above (Sahin et al. 2014; Weissman 2015). In this case, the genetic material is released directly into the cytoplasm of the host cell, where the translational machinery produces a sufficient amount of the mRNA-encoded immunogen which is afterward appropriately presented to the host immune system. For that reason, in vitro transcribed mRNA is much safer than DNA-based vaccines, with no risk of genomic integration and more efficient due to its reliance on the host's translational machinery. Moreover, delivery of such therapeutics is easier as mRNA can be translated immediately upon reaching cytosol with no need for nuclear transcription and subsequent export from the nucleus to the cytoplasm. Also, mRNA can be relatively easily produced in vitro, mainly by an in vitro transcription (IVT) reaction. This process, as well as the mRNA purification procedure, can be optimized independently of encoded antigens. Additionally, mRNA can be quite easily engineered to introduce modifications for different applications or to modulate its properties, for example, to increase translational efficiency or stability, which is not available for DNA vectors. One of the basic structural elements in mRNA that is required to keep mRNA functional and allows the improvement of mRNA properties is the 5′ end cap structure that consists of 7-methylguanosine connected via 5′–5′ triphosphate bridge to the first transcribed nucleoside (Furuichi

Corresponding author: marzena@chem.uw.edu.pl
Article is online at http://www.rnajournal.org/cgi/doi/10.1261/rna.079460.122. Freely available online through the *RNA* Open Access option.

2015). Recognized by highly specialized cap-binding proteins, the cap is involved in a number of processes, including maturation, nuclear export, initiation of translation, and turnover of mRNA (Galloway and Cowling 2019). The cap has a variety of functions spanning every phase of mRNA metabolism, but from the standpoint of its use as an RNA-based vaccine, the most important functions are those that enhance the translation initiation and protect against the 5′-to-3′ exonucleolytic degradation. These abilities can be achieved by introduction of modified cap analogs, the synthesis of which has been carried out for years. Initiation of translation is increased by cap analogs with a higher affinity to eukaryotic translation initiation factor 4E (eIF4E). Additionally, the mRNA stability is increased by modifications in the phosphate chain of the cap structure that make mRNA resistant to decapping enzymes, thus increasing the lifetime of mRNA in the cell (Ziemniak et al. 2013; Strenkowska et al. 2016). The most common capping method of transcripts is the incorporation of the dinucleotide cap analog (e.g., m^7GpppG/A) by RNA polymerase (e.g., T3, T7, or SP6) during IVT reaction. As a result, a functional mRNA with a properly integrated cap can be obtained together with the one that is built in reversed orientation. Anti-reverse cap analogs (ARCA) possessing the methyl group at the C2′ or C3′ position of 7-methylguanosine were the first dinucleotide caps that allowed proper incorporation during IVT (Grudzien-Nogalska et al. 2007). This modification also modulates the network of cap interactions with various proteins and thus positively affects the overall level of translation (Miedziak et al. 2019). It is not surprising that 3′-*O*-methylation of m^7G ribose has also been used in the cap analog applied in currently used mRNA vaccines against COVID-19 (Sahin et al. 2020). In order to increase the translation efficiency, caps with various modifications have been tested. One of the most effective so far has been the analogs obtained and tested in our previous research (Kocmik et al. 2018). They contained two types of modifications within m^7G: either 3′- or 2′-*O*-methylation and additionally a substitution at the N2 position (benzyl or 4-methoxybenzyl). The latter modification makes even monophosphates (N2 modified m^7GMPs) good translation inhibitors comparable to m^7GTP, as we have shown in in vitro studies in a cell-free reticulocyte system (RRL) (Piecyk et al. 2014). The data obtained identified the analog containing N2 benzyl and C2′ methoxy substituents as the most promising, since it showed increased expression levels both in vitro in RRL and in HEK293 cells. Furthermore, with the strongest inhibitory properties of cap-dependent translation (IC_{50} = 1.7 μM), this analog indirectly influenced the transcript stability compared to transcripts capped with m^7GpppG or $m_2{}^{7,3,O}$GpppG.

Within this work we describe the continuation of our previously published research with the use of a wider range of cap analogs modified only at the exocyclic amine group. Selected substituents include both benzyl derivatives (methoxy-, chloro-) as well as those with more extensive side chains such as appropriately substituted triazole, isoxazole or thiazole. The results of biological experiments have shown that cap analogs modified at the N2 position of 7-methylguanosine are extremely potent inhibitors of translation. They also represent an interesting component for incorporation in place of the standard mRNA cap. One of the new compounds was not only efficiently attached to the transcript, but also guaranteed the incorporation of cap analogs into mRNA only in the correct orientation. So far, ensuring the correct orientation of the incorporation is only possible with ARCA-type analogs or trinucleotides with A at position +1. Therefore, the presented compound represents a new alternative to the abovementioned ones. All the newly synthesized cap analogs enabled highly efficient translation of mRNA both in the in vitro translation system and in the human HEK293 cell line.

RESULTS

Chemistry

We present a series of N2-modified dinucleotide cap analogs prepared as substrates for 5′ capping of in vitro transcribed RNA (Fig. 1). Compounds 1–3 were synthesized previously for a different purpose (Piecyk et al. 2015). For the synthesis of the rest of the remaining dinucleotide cap analogs, a reliable, efficient and common method for the synthesis of a standard cap analog such as m^7GpppG was used (Kadokura et al. 1997). As was previously described, it requires an intermediate, imidazolide derivative of GDP that has been achieved through regioselective reaction of GDP with imidazole (Jemielity et al. 2003) under aqueous conditions and the coupling reaction of obtained derivative with appropriate N2-modified 7-methyl monophosphate (x^2m^7GMP), using the $ZnCl_2$/DMF system. N2-substituted 7-methylguanosine 5′-monophosphates corresponding to compounds 4–5 and P-imidazolide of guanosine 5′-diphosphate (GDP-Im) were synthesized according to the previously described protocols (Piecyk et al. 2014, 2020b). As the synthesis of thiazole N2-substituted 7-methylguanosine-5′-monophosphate has not been performed so far, it is depicted in Scheme 1 and described in detail in the Materials and Methods section. Dinucleotides were isolated from the reaction mixtures by ion-exchange chromatography on a DEAE Sephadex A-25 (HCO_3^- form) column. The final compounds were additionally purified using semipreparative RP-HPLC equipped with a C8 RP HPLC column and isolated from the eluate by repeated freezing-drying procedure. The structure and homogeneity of each compound was confirmed by rechromatography by RP-HPLC, high-resolution mass spectrometry using positive electro spray ionization (HRMS-ESI) and ^{1}H and ^{31}P NMR.

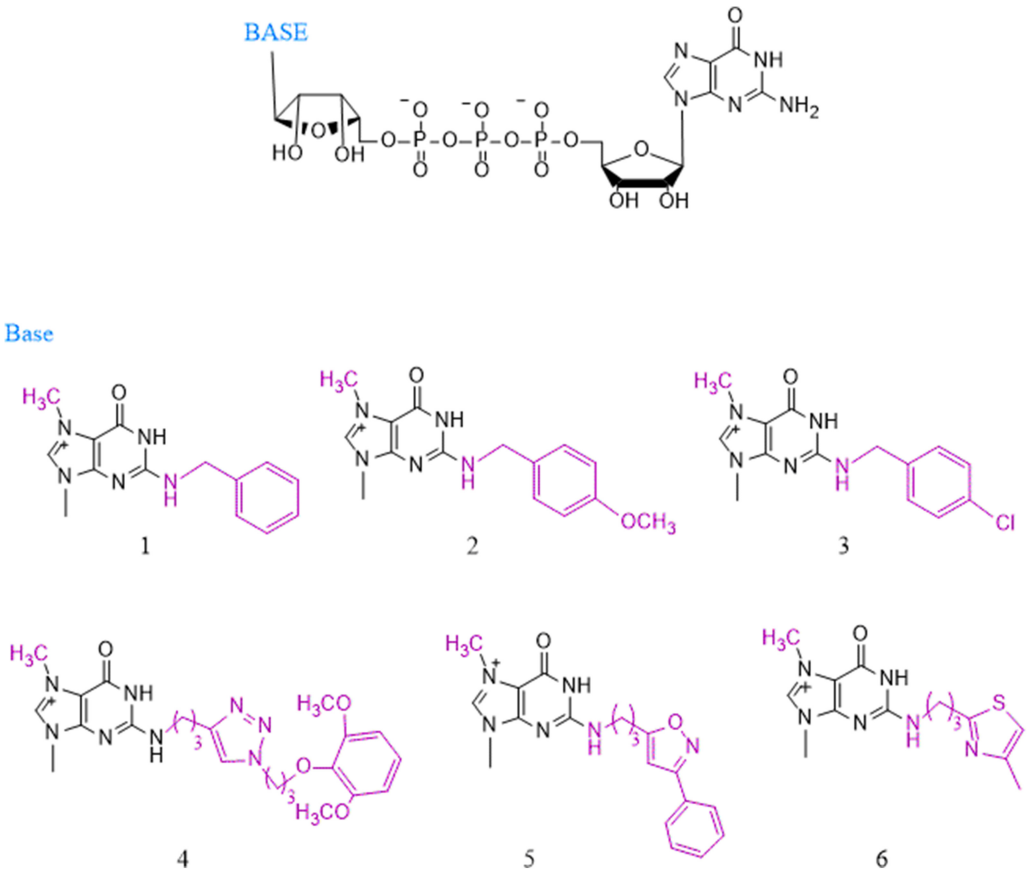

FIGURE 1. Structures of dinucleotide cap analogs synthesized and examined in this work.

Inhibitory potential

The ability of new cap analogs to inhibit cap-dependent translation in RRL system was determined. In order to obtain IC_{50} values, the translation efficiency for $m_2^{7,3'O}$GpppG-RNA encoding the firefly luciferase reporter protein was measured in the presence of increasing concentrations of a given cap analog. The obtained values are summarized in Table 1 and Figure 2. (4-bn-isx)^{2}m^{7}GpppG (5) and bn^{2}m^{7}GpppG (1) showed the best inhibitory properties (IC_{50} of 0.57 and 0.61 μM, respectively). Slightly weaker translational inhibitors were (4-OCH$_3$bn)^{2}m^{7}GpppG (2) and (4-Cl-bn)^{2}m^{7}GpppG (3), with IC_{50} values of 0.89 and 0.98 μM. The weakest inhibitors in this group were (4-(diOCH$_3$-bn)-tz)^{2}m^{7}GpppG (4) and (4-CH$_3$-th)^{2}m^{7}GpppG (6), although still with 6.9 and 4.8 times stronger inhibitory potential relative to the control m^{7}GpppG, respectively.

Efficiency and orientation of incorporation of cap analogs into mRNA

Next, we investigated whether the newly synthesized cap analogs are potent substrates for RNA polymerase for in vitro transcription and the efficiency of their incorporation into RNA. For this purpose, short RNA$_{25nt}$ was IVT synthesized; samples were separated on denaturing 16% UREA-PAGE (Fig. 3), where capped oligonucleotides (band C) migrate more slowly than the uncapped (band D) IVT products. As is seen, all tested analogs are efficiently incorporated into RNA transcripts by RNA polymerase. The percentage of the band containing capped RNA and uncapped pppRNA was evaluated densitometrically (similarly to that described by Vlatkovic et al. 2022). Among the control RNAs, the fraction containing the capped product was 85.3 ± 0.8% for GpppG-RNA, 74.3 ± 3.5% for m^{7}GpppG-RNA, and 65.8 ± 2.4% for $m_2^{7,3'O}$GpppG-RNA. The newly synthesized compounds (5), (3), and (1) were the most readily incorporated into RNA—the capped fraction constituted 88.5 ± 2.0%, 88.2 ± 4.6%, and 80.5 ± 1.6%, respectively. The fraction capped with analogs (4-OCH$_3$bn)^{2}m^{7}GpppG (2) and (6) was 77.3 ± 0.3% and 75.9 ± 2.2%. In contrast, compound (4), similarly to $m_2^{7,3'O}$GpppG, incorporated into RNA with greater difficulty; its capped fraction was estimated to be 67.5 ± 0.7%.

Only RNAs that have cap analogs exposing methylated m^{7}G at the 5′ end are translationally active in the cap-dependent process in the cell. To study the functionality of RNAs modified with the new compounds, we tested in which orientation they are built into RNA.

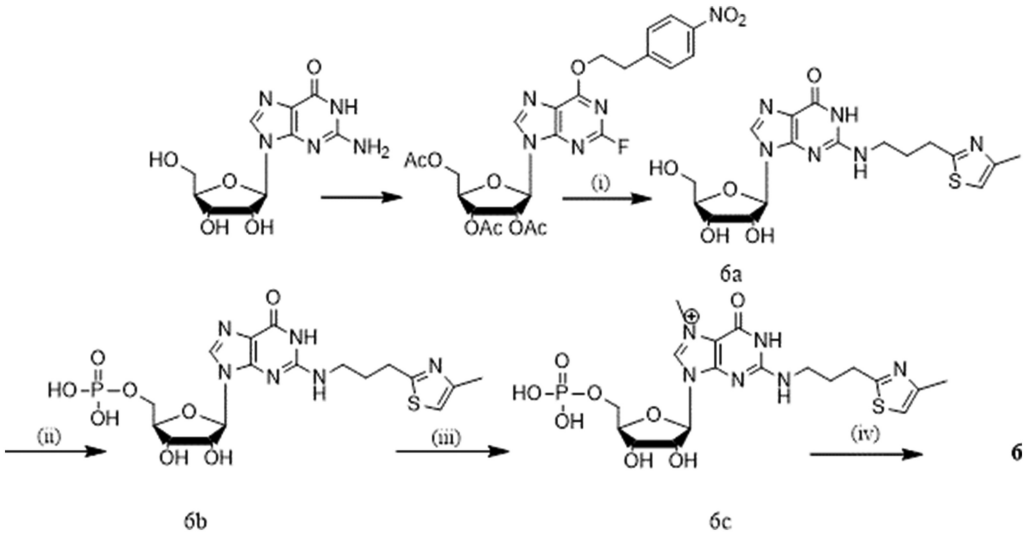

SCHEME 1. Synthesis of N2-(3-(4-methylthiazol-2-yl)propyl)-7-methylguanosine-5′-P^3-guanosine-5′-triphosphate (6); (i) 3-(4-methylthiazol-2-yl) propyl-1-amine, DMSO (ii) trimethyl phosphate, $POCl_3$ (iii) CH_3I, DMSO, (iv) guanosine 5′-diphosphate imidazolide, $ZnCl_2$, DMF.

We have taken advantage of the human hNudt16 enzyme that exhibits different hydrolytic specificity in regards to methylation status of the substrate. Previous studies have shown that this enzyme can hydrolyze, when used at higher concentrations, nonmethylated GpppG dinucleotide alone as well as GpppG attached to RNA chains, even though they are probably not its specific substrates. In contrast, compounds methylated at the N7 position are very poorly, or even not at all, hydrolyzed by hNudt16 (Grzela et al. 2018; Chrabąszczewska et al. 2021). Thus, in the developed here a "cap-orientation test," hNudt16 should target preferentially a nonmethylated 5′ end of the RNA transcript (that results from incorrect orientation of the incorporated cap dinucleotide), leaving intact the transcript with cap in the correct orientation (with exposed N7-methylguanosine). As a result, the higher fraction of transcripts with incorrectly oriented caps the more of hNudt16 decapped product should be detected.

Firstly, as a proof of concept, we performed hNudt16 hydrolysis of RNA_{25} capped with control analogs GpppG, m^7GpppG and $m_2^{7,3'O}$GpppG. Incubation with hNudt16 showed significant differences in the amount of decapped product (Fig. 3). For GpppG-RNA, the decapped band accounted for 86.2 ± 3.9% of the total reaction product. Incubation of $m_2^{7,3'O}$GpppG-capped RNA with hNudt16 accounted for only 8.7 ± 2.0% of the reaction product. In contrast, for m^7GpppG-RNA the decapped band amounted to 45.7 ± 3,4% of the product. As expected because hNudt16 is preferentially active against unmethylated GpppG-RNA, it was almost completely decapped. In contrast, as the $m_2^{7,3'O}$GpppG cap is almost exclusively incorporated into RNA transcript in the correct orientation, and the methylated part of the analog is available to the Nudt16 enzyme, the very poor progress of the decapping reaction was achieved. Finally, the RNA capped with m^7GpppG is a mixture of two products m^7GpppG-RNA and Gpppm^{7}G-RNA of which only that with the terminal unmethylated guanosine is hydrolyzed by hNudt16. Therefore, only half of the material in this sample was hydrolyzed. Thus, the hNudt16 enzyme proved to be a good tool to estimate the percentage of unmethylated fraction of RNA in IVT samples. Moreover, the orientation of the incorporation of the cap analog can be indirectly deduced from the data obtained in the applied approach. Our results also indicate that the correct orientation of the cap analog is associated with lower overall efficiency of incorporation of the compound into RNA.

Prior to investigating the sensitivity of RNAs containing newly synthesized cap analogs to hNudt16 hydrolysis, we also checked whether any of the modifications introduced to the cap could constitute a steric hindrance for the decapping enzymes, thus preventing the progress of the reaction. We tested them in reaction with the major decapping enzyme—hDcp2—that, similarly to hNudt16,

TABLE 1. Inhibition of ARCA-mRNA luciferase translation in RRL system

Cap analog	IC_{50} (μM)
m^7GpppG	8.94 ± 0.86
bn^{2}m^{7}GpppG (1)	0.61 ± 0.04
(4-OCH$_3$bn)^{2}m^{7}GpppG (2)	0.89 ± 0.12
(4-Cl-bn)^{2}m^{7}GpppG (3)	0.98 ± 0.13
(4-(diOCH$_3$-bn)-tz)^{2}m^{7}GpppG (4)	1.30 ± 0.23
(4-bn-isx)^{2}m^{7}GpppG (5)	0.57 ± 0.06
(4-CH$_3$-th)^{2}m^{7}GpppG (6)	1.87 ± 0.08

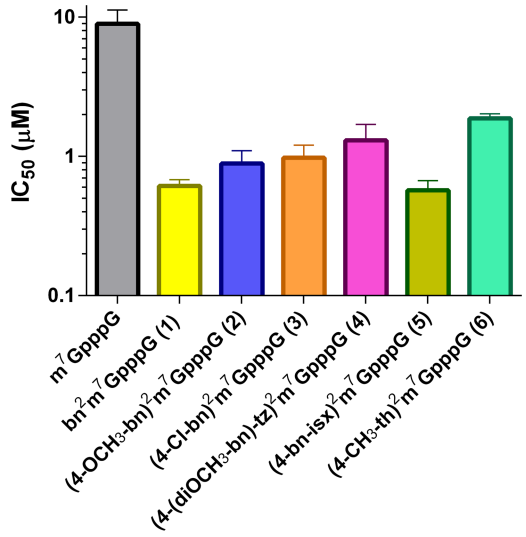

FIGURE 2. Inhibition of ARCA-mRNA luciferase translation in RRL system.

utilize the NUDIX motif in enzymatic activity and hydrolyze the triphosphate chain at the same site (Chrabąszczewska et al. 2021). As shown in Figure 3, within 30 min of reaction, hDcp2 was able to hydrolyze the cap of every analog-capped mRNA under experimental conditions with 100% efficiency, demonstrating that the triphosphate chain in all newly synthesized analogs with N2 substitutions is not blocked from the enzyme activity.

Next, we investigated the progress of hNudt16 hydrolysis reaction of RNAs capped with the newly synthesized cap analogs (1–6) in the "cap-orientation test." In each case, replacement of the GpppG cap with the newly synthesized cap analog resulted in increased oligonucleotide stability relative to hNudt16 activity (Table 2; Fig. 4, left panel). The level of cap hydrolysis of (4-(diOCH$_3$-bn)-tz)^{2}m^{7}GpppG-capped RNA (7.6 ± 1.7) was comparable to that obtained for m$_2^{7,3'O}$GpppG-capped transcripts (8.7 ± 2.0). For the other analogs (1, 2, 3, 5, and 6), the amount of hydrolyzed product ranged between 21.2 ± 5.8% and 33.3 ± 7.2% (Table 2; Fig. 4, left panel). These results indicate the presence of a negligible fraction of unmethylated RNA in the (4-(diOCH$_3$-bn)-tz)^{2}m^{7}GpppG-capped sample. Also, other RNAs capped with the new analogs showed a reduced presence of unmethylated transcripts compared to the control m^{7}GpppG-RNA.

The above results suggest that, in the case of new cap analogs, SP6 polymerase preferentially attacks the 3′-OH group on the unmodified guanosine side. This is particularly prominent for mRNA capped with (4-(diOCH$_3$-bn)-tz)^{2}m^{7}GpppG (4), where the negligible fraction of detected decapped product indicates that the dinucleotide can be elongated into the RNA chain exclusively on the unmethylated G side the [and not at the (4-(diOCH$_3$-bn)-tz)^{2}m^{7}G side]. We tested this finding also for T7 RNA polymerase—another enzyme used extensively in preparations of (m)RNAs in IVT reactions (Milligan et al. 1987). We prepared RNA transcripts capped with control cap analogs and with compound (4) in reaction with T7 RNA polymerase, and then treated them with hNudt16 as described above (Table 2; Fig. 4, right panel). The hydrolysis product constituted 82.06% for GpppG-RNA, 32.25% for m^{7}GpppG-RNA, and 4.81% for m$_2^{7,3'O}$GpppG-RNA. (4-(diOCH$_3$-bn)-tz)^{2}m^{7}GpppG-capped RNA was hydrolyzed at the rate similar to m$_2^{7,3'O}$GpppG-RNA—the hydrolysis product at the end of the reaction was only 2.74%. These results indicate that the modification at position N2 of m^{7}G affects the orientation of cap analog incorporation into RNA by both RNA polymerases.

Thermal stabilization of eIF4E in the presence of newly synthesized ligands

Since the obtained analogs showed interesting properties and could therefore be an appealing alternative to the currently known and used ones, we decided to characterize them in detail. Among the desirable features is the high

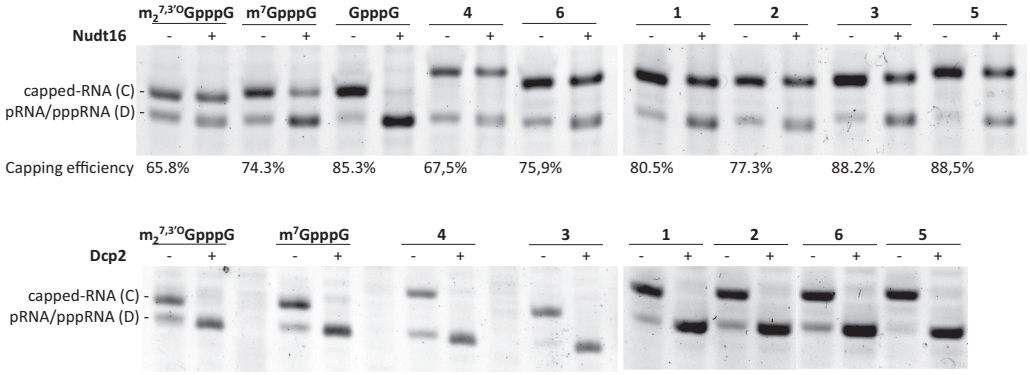

FIGURE 3. 5′ cap hydrolysis of analog-capped mRNAs with hNudt 16 (*A*) and hDcp2 (*B*). Gel electrophoretic analysis of decapping of analog-capped RNA$_{25}$. Analog-capped (1–6) RNA$_{25}$ were subjected to 30 min incubation with hNudt16 and hDcp2 and run on denaturing 15% polyacrylamide/7 M urea gel. C indicates the capped product that did not undergo hydrolysis, and D indicates the oligonucleotide without the cap. The decapped product at time 0 results from the incomplete capping during the IVT reaction.

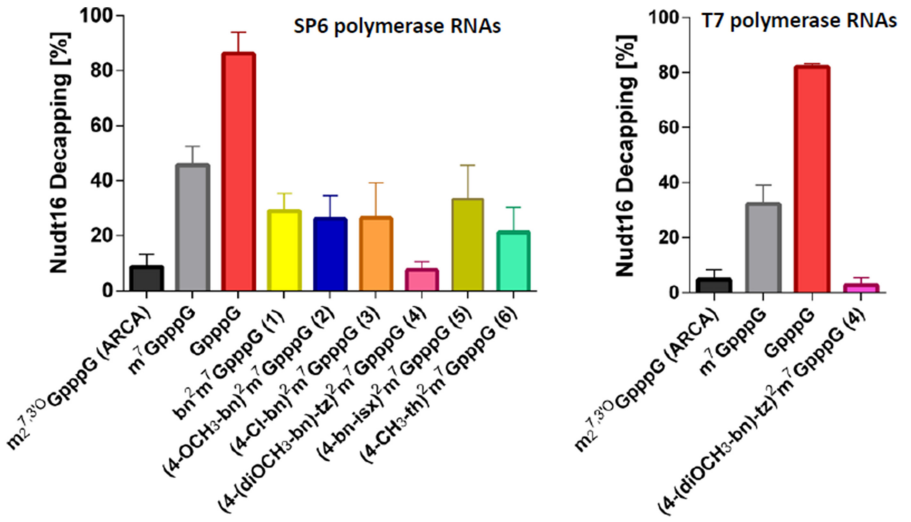

FIGURE 4. The level of 5′ cap hydrolysis of analog-capped mRNAs with hNudt16. The graph represents the percentage of mRNA (in vitro synthesized in reaction with SP6 polymerase on the *left* or with T7 polymerase on the *right*) that underwent the cap hydrolysis in 30 min reaction with hNudt16. The level of hydrolysis was calculated on the basis of densitometric analysis as the percent loss in the capped band after addition of the enzyme. Data represent the mean ± SD of at least three independent experiments.

translational efficiency, dependent on the eIF4E protein. Thus, our next step was to investigate the interaction between the newly synthesized cap analogs and the eIF4E protein. To characterize the affinity of newly synthesized compounds to the eIF4E translation initiation factor, the thermal stability of murine eIF4E (98% identical to human homolog) (Volpon et al. 2006) in their presence was analyzed with the DSF approach (Niesen et al. 2007). As shown in Figure 5, at the same ligand concentration for the standard dinucleotide cap analogs m^7GpppG and $m_2^{7,3'O}$GpppG, a distinct stabilization reflected with DSF melting profiles a positive shift (around 10°C) in relation to the unbound (apo) form of eIF4E is seen. Nonfunctional cap analog ApppG does not stabilize eIF4E in the same experimental conditions at all. Modifications introduced into new cap analogs studied here resulted in compounds that have an even better positive effect on the thermal stability of eIF4E (up to around a 14°C increase in T_m in the presence of (4-bn-isx)$^2m^7$GpppG) (5), and thus bind the protein with similar/or better affinity than m^7GpppG and $m_2^{7,3'O}$GpppG. Estimated apparent affinity (*app.*K_d) based on the T_m change in response to the increasing concentrations of the analyzed ligand (Supplemental Figs. S7, S8), revealed that the above-mentioned compound (4-bn-isx)$^2m^7$GpppG (5) and (4-Cl-bn)$^2m^7$GpppG (compound 3) have around 5× higher affinity to eIF4E in comparison to m^7GpppG (Table 3). Affinities of remaining new compounds are around 2.5 times higher [in the case of analogs 1 and (4-OCH_3bn)$^2m^7$GpppG (2)] and around 1.7 times higher for analogs (4-CH_3-th)$^2m^7$GpppG (6) and (4-(diOCH_3-bn)-tz)$^2m^7$GpppG (4).

Expression level in RRL

The newly synthesized cap analogs were used in IVT preparations of mRNA encoding the firefly luciferase (reporter protein) in order to investigate their effect on the level of protein translation in RRL system. Three control mRNAs capped with m^7GpppG, $m_2^{7,3'O}$GpppG, and ApppG were included in this study. The translation efficiency of the $m_2^{7,3'O}$GpppG-capped transcript was 1.47-fold higher

TABLE 2. 5′ cap hydrolysis of analog-capped mRNAs with hNudt16

Cap analog	% of hydrolysis SP6 product	SD	% of hydrolysis T7 product	SD
$m_2^{7,3'O}$GpppG (ARCA)	8.72	2.04	4.81	1.82
m^7GpppG	45.74	3.42	32.24	3.40
GpppG	86.18	3.93	82.06	0.60
bn$^2m^7$GpppG (1)	29.05	3.72	n.d.	n.d.
(4-OCH_3bn)$^2m^7$GpppG (2)	26.09	4.21	n.d.	n.d.
(4-Cl-bn)$^2m^7$GpppG (3)	26.45	7.34	n.d.	n.d.
(4-(diOCH_3-bn)-tz)$^2m^7$GpppG (4)	7.64	1.71	2.74	1.35
(4-bn-isx)$^2m^7$GpppG (5)	33.25	7.16	n.d.	n.d.
(4-CH_3-th)$^2m^7$GpppG (6)	21.2	5.28	n.d.	n.d.

The table represents the percentage of mRNA that underwent the cap hydrolysis in 30 min reaction with hNudt16 calculated on the basis of densitometric analysis as the percent loss in the capped band after addition of the enzyme. Data represent the mean ± SD of at least three independent experiments.

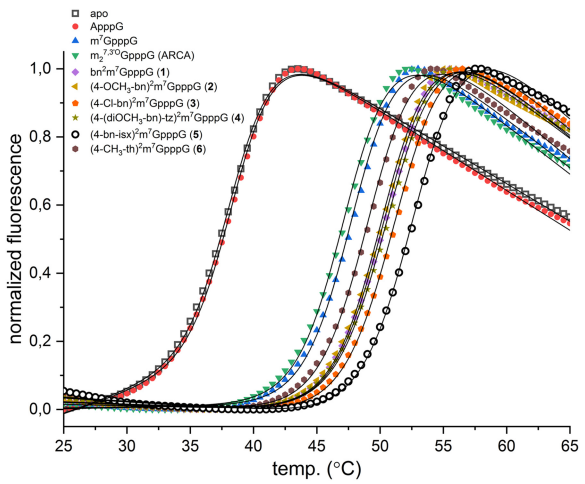

FIGURE 5. Analysis of thermostability of eIF4E translation factor by DSF in the presence of examined cap analogs. Representative DSF melting profiles of murine eIF4E alone (open squares, □) and in the presence of 100 μM of standard compounds: ApppG, m^7GpppG, and $m^{7,3'O}$GpppG (ARCA), or newly synthesized compounds 1–6. Measured DSF fluorescence signal was normalized and used to calculate T_m values with CDpal (fitted lines) (Niklasson et al. 2015). As is shown, ApppG does not stabilize eIF4E (negative control), and m^7GpppG and $m^{7,3'O}$GpppG standard dinucleotide cap analogs increase the eIF4E thermal stability to the same extent (T_m value around 10°C higher in comparison to apo form). All newly synthesized compounds stabilize eIF4E even better than standard cap analogs (T_m values higher more than 10°C), and compound 5 (open circles, ○) gives the highest shift of the DSF melting curve and the increase of the T_m value around 15°C.

than that of the m^7GpppG-capped transcript, and mRNA capped with nonfunctional ApppG was translated at a very low level (at ~10% in comparison to m^7GpppG-capped transcript) (Table 4), which is consistent with conditions for cap-dependent translation and previously published data (Jemielity et al. 2003). Among the tested mRNAs, those capped with (4-bn-isx)$^2m^7$GpppG (5), bn$^2m^7$GpppG (1), or (4-Cl-bn)$^2m^7$GpppG (3) showed more than three times higher translational activity than that obtained for m^7GpppG-RNA. The other two compounds: (4-OCH_3bn)$^2m^7$GpppG (2) and (4-(diOCH_3-bn)-tz)$^2m^7$GpppG (4) had slightly lower translation efficiency, but still 2.65 and 2.76 times higher than the control m^7GpppG-RNA. Analog (4-CH_3-th)$^2m^7$GpppG (6) showed 1.92 times higher translation efficiency than m^7GpppG-RNA.

Translational properties in HEK293 cells

Further, we tested the expression level of mRNAs capped with the newly synthesized cap analogs in a more complex cellular environment, that is, in HEK293 cells. Firefly luciferase encoding mRNAs with modified caps were obtained as previously in an IVT reaction, polyadenylated and transfected in equal amounts to HEK293 cells. The translation efficiency was measured 6, 12, 24, and 48 h post transfection as the relative luciferase activity (Fig. 6A). The relative total luciferase expression was defined as the integral of the curve normalized to the value obtained for m^7GpppG-capped mRNA (Table 4; Fig. 6B). The highest total protein expression result (increased by factor 2.3 ± 0.1) was obtained for (4-Cl-bn)$^2m^7$GpppG (3), which was among the top three of the mRNAs tested in the RRL assay. The RNAs capped with compounds bn$^2m^7$GpppG (1), (4-OCH_3bn)$^2m^7$GpppG (2), (4-(diOCH_3-bn)-tz)$^2m^7$GpppG (4) and (4-bn-isx)$^2m^7$GpppG (5) gave very similar results (1.80 ± 0.34, 2.2 ± 0.9, 2.0 ± 0.1, and 1.6 ± 0.1, respectively), the total protein expression in this group was increased by 1.6–2.2-fold compared to the standard m^7GpppG-RNA. The weakest benefit was observed in translation of RNA capped with compound (4-CH_3-th)$^2m^7$GpppG (6)—1.4 ± 0.2.

DISCUSSION

Recent years with the SARS-CoV-2 pandemic brought a technological revolution in the field of drugs based on the mRNA molecule. In 2020, the first mRNA-based drug, the COVID-19 vaccine, was launched in the pharmaceutical market after successfully passing the various stages of clinical trials (Polack et al. 2020; Baden et al. 2021). The use of a preventive drug on a global scale in both adults and children undeniably demonstrates the safety and effectiveness of the mRNA molecule as a carrier of genetic information. This spectacular success of mRNA is in fact only the beginning of the exploration of the potential inherent in this molecule. It is believed that the coming years will bring a rapid development of mRNA-based drugs to fight a variety of diseases. Currently, many scientific and preclinical studies are focused on discovering ways to provide this molecule with even better properties than before. Our research is part of this global trend in the development of a more functional mRNA molecule. One strategy for modifying mRNA is to replace the cap structure at its 5′ end with a modified cap analog. The synthesis of chemical analogs of the cap is a very important field of therapeutic mRNA research, and has so far enabled significant stabilization of this molecule and improvement of its translational efficiency. In this work, we report the chemical synthesis and biochemical characterization of the new class of RNA capped with six dinucleotide cap analogs containing only a single aromatic substituent at the N2 position of 7-methylguanosine.

Cap analogs have a dual therapeutic potential. As mentioned above, they can be incorporated into the mRNA molecule as an important part of it, but they can also be used independently. A cap analog with high affinity for translation initiation factors will preferentially bind to them, preventing mRNA binding. Such molecules are therefore inhibitors of translation, and their development is important for anticancer therapies. Therefore, all newly synthesized cap analogs are routinely screened for their

TABLE 3. Summary of interaction analysis of new compounds with eIF4E by DSF approach

	1[a]		2[b]	3[c]	4
Compound	T_m (°C) (at 100 μM of ligand)	St. err. of mean	ΔT_m (at 100 μM of ligand)	*app.* K_d (μM)	Adj. R-square
None	38.42	0.05	-	-	-
ApppG	38.62	0.04	0.20	n.d.	-
m^7GpppG	48.10	0.02	9.68	14.01 (±2.69)	0.990
$m_2^{7,3'O}$GpppG	47.53	0.05	9.11	n.d.	-
bn^2m^7GpppG (1)	50.71	0.04	12.29	5.03 (±1.19)	0.985
(4-OCH_3-bn)$^2m^7$GpppG (2)	50.40	0.05	11.98	6.26 (±1.97)	0.974
(4-Cl-bn)$^2m^7$GpppG (3)	51.50	0.08	13.08	3.10 (±1.05)	0.974
(4-(diOCH_3-bn)-tz)$^2m^7$GpppG (4)	51.04	0.09	12.62	8.46 (±2.38)	0.978
(4-bn-isx)$^2m^7$GpppG (5)	52.95	0.03	14.53	2.61 (±1.01)	0.969
(4-CH_3-th)$^2m^7$GpppG (6)	49.49	0.08	11.07	7.99 (±1.47)	0.990

[a]Melting temperatures (T_m,°C) of murine eIF4E in the presence of 100 μM of studied compound. Presented values correspond to the arithmetic mean of two independent experiments (±SE of the mean). T_m values were calculated using CDpal software (Niklasson et al. 2015) and implemented the two-state protein denaturation model.

[b]ΔT_m (at 100 μM of ligand)—in relation to eIF4E in apo form.

[c]*app.*K_d (μM)—apparent affinity, based on ΔT_m change in the presence of the increasing concentration of the analyzed ligand. Compound concentrations used in this experiment were as follows: 1, 2, 5, 10, 20, 40, and 100 μM for bn^2m^7GpppG (1), (4-Cl-bn)$^2m^7$GpppG (3), (4-bn-isx)$^2m^7$GpppG (5), and (4-CH_3-th)$^2m^7$GpppG (6), and 2,5,10,20,40,100 μM for (4-OCH_3-bn)$^2m^7$GpppG (2), (4-(diOCH_3-bn)-tz)$^2m^7$GpppG (4), and m^7GpppG. T_m values were calculated using CDpal software, and obtained ΔT_m data were plotted versus corresponding concentration (in μM) of analyzed compound (Supplemental Figs. S7, S8), and *app.*K_d were calculated by fitting the single site ligand binding model function (Vivoli et al. 2014), using Origin Pro software. Presented here are *app.*K_d values that correspond to the single experiment.

inhibitory properties in the cell-free in vitro translation system. The dinucleotide cap analogs that have been studied so far can be generally divided into three main groups: (a) analogs having modification within triphosphate bridge with or without ARCA modification, (b) analogs modified at the N7 position with or without ARCA modification, and finally (c) N2 modified ARCA cap analogs. In terms of N7 modified cap analogs, recently a broad range of N7-arylmethyl substituted analogs have been tested (Wojcik et al. 2021). Among seventeen novel caps, the most potent translation inhibitors were the ones having p-fluoro, p-bromo, m-methylbenzyl or unsubstituted benzyl groups with IC_{50} values 6.0 ± 0.9, 6.4 ± 1.0, 6.6 ± 0.8, 7.4 ± 1.4 μM, respectively, being around twofold more potent than m^7GpppG (IC_{50} 11.4 ± 2.4 μM). It should be mentioned, however, that among the whole set of tested analogs, around half of them (modified in the N7 position, e.g., with 2-methoxybenzyl, 4-nitrobenzyl, 4-chlorobenzyl substituents) were less effective than the standard m^7GpppG cap analog. These results clearly show that

TABLE 4. Translational properties of mRNA capped with the newly synthesized cap analogs in the RRL system and HEK293 cells

	Rabbit reticulocyte lysate		HEK293 cells
Cap analog	Relative translation efficiency	Relative cap-dependent translation efficiency	Relative total protein expression
$m_2^{7,3'-O}$GpppG	1.47 ± 0.17	1.53 ± 0.20	1.29 ± 0.25
m^7GpppG	1	1	1
ApppG	0.09 ± 0.06	0	0.45 ± 0.21
bn^2m^7GpppG (1)	3.30 ± 0.77	3.52 ± 0.82	1.80 ± 0.34
(4-OCH_3bn)$^2m^7$GpppG (2)	2.76 ± 0.54	2.94 ± 0.53	2.18 ± 0.91
(4-Cl-bn)$^2m^7$GpppG (3)	3.29 ± 0.74	3.52 ± 0.73	2.29 ± 0.12
(4-(diOCH_3-bn)-tz)$^2m^7$GpppG (4)	2.65 ± 0.89	2.80 ± 0.90	1.96 ± 0.05
(4-bn-isx)$^2m^7$GpppG (5)	3.37 ± 0.84	3.51 ± 0.82	1.64 ± 0.09
(4-CH_3-th)$^2m^7$GpppG (6)	1.92 ± 0.43	2.00 ± 0.44	1.42 ± 0.20

The level of total luciferase expression in HEK293 cells is depicted as the integral of the curve normalized to the value obtained for m^7GpppG-capped mRNA. Data represent the mean ± SD of six measurements with two independent mRNA preparations (three repeats from each mRNA preparation).

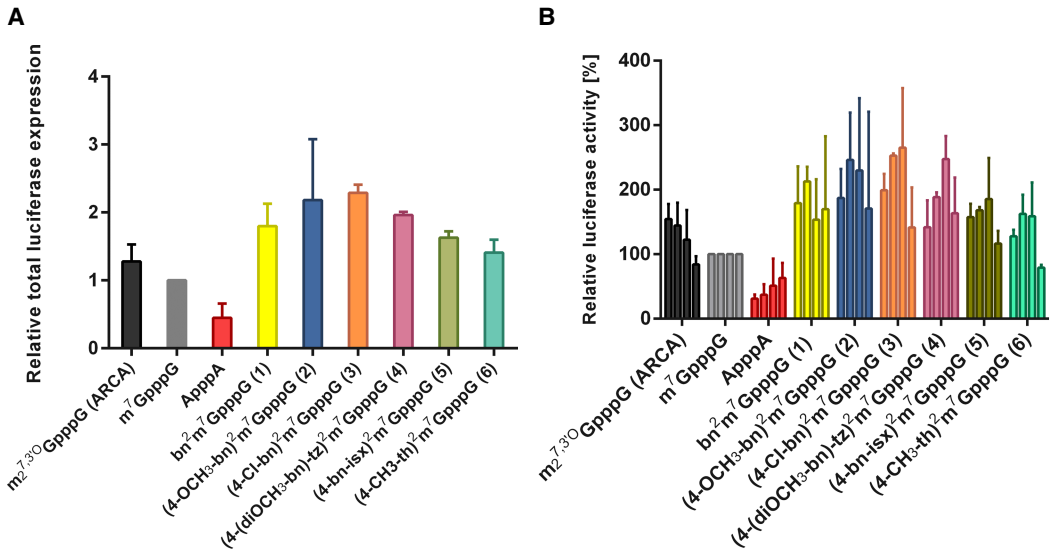

FIGURE 6. Translation efficiency of mRNAs capped with cap analogs (1–6) in HEK293 cells. (*A*) Translation level is presented as the relative luciferase activity after normalization to the protein concentration. (*B*) The level of total luciferase expression is depicted as the integral of the curve normalized to the value obtained for m^7GpppG-capped mRNA. Both graphs show the mean ± SD of at least two independent experiments, each consisting of three repeats.

the replacement of the methyl group by other substituents can be very important in the context of generating analogs with high inhibitory properties; however, it is difficult to unequivocally predict how the analogs with specific substituents will behave. In the above-mentioned paper, it was also shown that the addition of the methyl group at the 2′-*O*-position of 7-methylguanosine additionally enhanced inhibitory properties of selected analogs (i.e., analog with a p-chlorobenzyl substituent was about threefold worse and with benzyl about two times worse inhibitor than their 2′ARCA counterparts). Moving on and analyzing another group of compounds, a number of dinucleotide phosphate-modified cap analogs carrying single or multiple O-to-X substitutions within the tri- or tetraphosphate chain (where X is a single atom or a group of atoms) have been studied in the context of their inhibitory potential. As in the case of modifications in the N7 position, modifications within the phosphate bridge can either lead to improvement or deterioration of inhibitory properties (e.g., compounds containing a methylene bridge are twofold worse translational inhibitors than the standard cap analog, while the exemplary borate-phosphate or imidophosphates show enhanced inhibitory properties) (Kalek et al. 2011; Rydzik et al. 2012; Kowalska et al. 2014).

It was shown that ARCAs with a single phosphorothioate modification at either the β or γ position of the 5′,5′-triphosphate chain are strong inhibitors of translation being 1.4- to fourfold better than m7GpppG. At the same time, ARCAs with a double phosphorothioate modification—P1,P2-dithiophosphate diastereoisomers—are five to six times stronger than m7GpppG. The most potent inhibitors turned out to be tetraphosphates with double phosphate modifications—P1,P2- and P2, P3-dithiotetraphosphate counterparts up to 10-fold (Kowalska et al. 2008; Strenkowska et al. 2016).

In our research, we investigated triphosphate dinucleotide analogs with only a single aromatic substituent at the N2 position of 7-methylguanosine, and it turned out that all tested compounds were better inhibitors (from about five- to almost 16-fold) than a standard m^7GpppG cap. The best results were achieved for the derivatives containing isoxazole (5) and benzyl (1) substituents (15.7- and 14.7-fold lower IC_{50}) and those with p-chlorobenzyl (3) or p-methoxybenzyl (2) substituents which had only slightly higher IC_{50} but still approximately 10-fold better than the standard cap. These data indicate that the group of analogs examined has exceptionally favorable inhibitory properties compared to other compounds tested so far. What is interesting, two of above-mentioned compounds —with benzyl and methoxybenzyl substituents—were previously prepared and tested in the form of ARCA dinucleotide analogs. Comparing the results, it is noticeable that the presence of ARCA modification in combination with the one at N2 position leads to a reduction in the translation inhibition capacity. This can probably be explained by the fact that these two modifications create a steric hindrance compared to modifications at ribose (ARCA) and the N7 position (Wojcik et al. 2021) or phosphates chain (Strenkowska et al. 2016).

The IC_{50} values obtained from translation inhibition assay are consistent with the appK_d values calculated for eIF4E-cap analog complex in the DSF approach. All tested compounds gave lower dissociation constants than the one obtained for m^7GpppG. In particular, the lowest K_d

was achieved for compound substituted with isoxazole (5) and p-chlorobenzyl (3), slightly higher for benzyl (1) and methoxybenzyl (2) and the highest for compounds (4) and (6), although still lower than for m^7GpppG. Taken together, our data clearly show that compared to m^7GpppG, all newly synthesized analogs bind more strongly to eIF4E.

At this point, it is difficult to fully explain why aromatic substitutions at the N2 position of 7-methylguanosine have such a strong positive effect on the affinity of such analogs for eI4E and their inhibitory properties. It is known from previous studies (Cai et al. 1999; Niedzwiecka et al. 2002) that one methyl group at the N2 is well tolerated, but substitution of the nitrogen atom with two methyl groups as in the case of trimethylguanosine cap ($m_3^{2,2,7}$G) significantly reduces its affinity for eIF4E (several hundred times lower K_{as} for $m_3^{2,2,7}$GTP compared to m^7GTP), as well as its efficacy as a translation inhibitor. This is consistent with the three-dimensional structures of murine eIF4E bound to 7-methyl-GDP, which revealed the presence of a single H-bond between N2 and the carboxyl group of the Glu residue. The loss of this hydrogen bond at the $m_3^{2,2,7}$G cap is thought to weaker the binding to eIF4E. Because the exocyclic amino group is solvent exposed, aromatic substituents at this position may form additional interactions with eIF4E leading to conformational changes affecting the binding pocket and/or the thermodynamics of the binding process.

Further studies were pursued to test the new cap analogs as a part of the mRNA molecule encoding the luciferase reporter protein. We demonstrated that the new cap analogs are efficiently incorporated into mRNA by RNA polymerases although with a slightly different score. For the two analogs, (4-bn-isx)^{2}m^{7}GpppG (5) and (4-Cl-bn)^{2}m^{7}GpppG (3), the fraction of capped mRNA was nearly 90%. We noted that the $m_2^{7,3'O}$GpppG analog was inserted into mRNA with lower efficiency of ~66% and among the new analogs, one, e.g., (4-(diOCH$_3$-bn)-tz)^{2}m^{7}GpppG (4), was incorporated with a comparable efficiency of 67.5 ± 0.7%.

SP6 and T7 RNA polymerases can initiate the transcription reaction in the presence of m^7GpppG analogs and their derivatives, both by attacking the 3′-OH group of guanosine as well as m^7G. This results in a mixture of transcripts having m^7GpppG-RNA and Gpppm^{7}G-RNA at the 5′ end (Pasquinelli et al. 1995). The latter product is translationally inactive and greatly reduces the amount of heterologous protein produced from RNA preparation. The problem of reverse incorporation of cap analogs has been solved by chemical methylation of the 3′-*O* or 2′-*O* position of m^7G. ARCA analogs containing such modifications are incorporated only in the correct orientation (Stepinski et al. 2001; Peng et al. 2002; Jemielity et al. 2003). However, as we noted, the correct orientation of the incorporation slightly decreases the overall insertion efficiency.

Since the orientation of incorporation is an important factor determining the expression level of the transcript, we tested all new analogs in this regard. For this purpose, we used the enzyme hNudt16, whose hydrolytic activity is dependent on the lack of methylation at the 5′ end of the mRNA. Current methods for assessing incorporation are laborious and often require radioactive labeling of cap analogs, which is difficult to achieve, especially when whole series of analogs are synthesized. However, the developed assay is based on a one-step enzymatic reaction to determine which end of the dinucleotide is exposed.

Control measurements with standard cap analogs confirmed the suitability of the hNudt16 enzyme used for this assay. Unmethylated GpppG-RNA was rapidly hydrolyzed in the triphosphate chain, whereas $m_2^{7,3'O}$GpppG-RNA was hydrolyzed only to a minor extent. m^7GpppG, which is incorporated in two orientations, was hydrolyzed with an efficiency close to 50%. Among the newly synthesized cap analogs, (4-(diOCH$_3$-bn)-tz)^{2}m^{7}GpppG (4) behaved very similarly to $m_2^{7,3'O}$GpppG. When RNA capped with this compound was treated with hNudt16, the reaction progress was very slow. This suggests that analog (4) was incorporated, like $m_2^{7,3'O}$GpppG, only in the correct orientation. Interesting results were obtained for RNAs capped with the rest of the compounds (1, 2, 3, 5) and (6). Although RNAs containing these caps were hydrolyzed with hNudt16, the progress of these reactions was slower than hydrolysis of m^7GpppG-capped RNA. This indicates that the modifications introduced on the N2 guanosine increase the probability of cap incorporation in the correct orientation. The same results were observed for cap incorporation with the use of T7 RNA polymerase. Taking into account the above results, we may assume that the correct orientation of the incorporation is associated with lower reaction efficiency. This is probably due to some steric difficulty for RNA polymerase as it can only attack the 3′-OH group from one side of the dinucleotide.

This is coherent with the finding that certain mononucleotide modifications significantly affect their incorporation by RNA polymerases into the body of the transcript (Suydam and Strobel 2009). It has been shown that the incorporation of mononucleotides with modifications at the 2′-deoxy- and 2′-*O*-methyl- ribose or N2-methylguanosine positions into the RNA chain is difficult for T7 RNA polymerase. The Y639F point mutation of T7 polymerase is required for this process to be efficient, often in combination with increased concentration of the modified analog and decreased concentration of unmodified NTPs. Tyr639 lies within the active site of the enzyme and has the ability to sense abnormal geometry in the substrate structure. Its substitution to Phe relaxes the substrate specificity of T7 RNA polymerase. Thus, Tyr639 has a specialized role in controlling the correct structure of the incorporated

substrate (Sousa and Padilla 1995). Both Tyr639 and the nearest amino acids are tightly conserved in the sequence of both T7 and SP6 polymerases (Tyr639 indicated by an arrow and the nearby fragment by a black box in the Supplemental Fig. S9). This is therefore not surprising that dinucleotide analogs having 2′-deoxy and 2′-*O*-methyldeoxyribose on one side are incorporated into the RNA chain only on the other side of the unmodified nucleoside.

Our results show, for the first time, that dinucleotides modified at the N2-methylguanosine position can behave as antireverse cap analogs. The presence of such a modification makes it more difficult for the RNA polymerase to attack from the modified dinucleotide side and has a positive effect on the orientation of the dinucleotide incorporation. For some substituents, this modification is sufficient for the analog to be incorporated solely in the correct orientation.

In order to evaluate preliminarily the functionality of RNA capped with N2 analogs, we examined the expression level of the transcripts in the RRL system. In our experiments, the relative translation efficiency for the control $m_2^{7,3'O}$GpppG-capped RNA was 1.47-fold higher than for the m^7GpppG-capped transcript, which is consistent with previously obtained values for $m_2^{7,3'O}$GpppG-capped mRNA (Jemielity et al. 2003). This effect was explained by correct incorporation of ARCA analogs in 100% of translationally active mRNA. All tested analogs incorporated into mRNA led to a 1.9- to 3.4-fold increase in translation efficiency than that achieved for the standard m^7GpppG cap (Table 4). Analogs that particularly caught our attention were: compounds (5), (1) and (3) with isoxazole, benzyl and p-chlorobenzyl substituents, respectively, for which mRNAs were translated with an efficiency more than 3.3-fold higher compared to m^7GpppG and about twofold higher than for $m_2^{7,3'O}$GpppG. Interestingly, these analogs at the same time presented the highest affinity for the eIF4E protein (Table 3), as well as the highest potential as inhibitors of the translation process in RRL (Table 1). Moreover, the above-mentioned analogs were incorporated into the transcripts during IVT with 80%–88% yield. At this point it should be mentioned that, compared to other tested compounds, the preference for incorporation into mRNA in the correct orientation was lower (~60%–74%). The analog (6) with the thiazole substituent showed the lowest translation efficiency but still twofold higher than m^7GpppG. As could be expected, compound (6) had the lowest affinity to eIF4E and was the weakest inhibitor of translation in the RRL. It is interesting to compare the results gathered for analogs bn^2m^7GpppG (1), and (4-OCH_3bn)$^2m^7$GpppG (2) with the results obtained previously for ARCA analogs containing benzyl and p-methoxybenzyl substituents at the N2 position. It was shown that such analogs introduced into mRNA led to the 1.3–1.4 times more efficient translation compared to m^7GpppG-capped RNA (Kocmik et al. 2018). What is interesting, the new compounds (1) and (2) without ribose modification incorporated into mRNA allowed for approximately threefold increase in translation efficiency. The same observation was made when analyzing inhibitory properties of cap analogs. We therefore postulate that in the case of N2 modifications the presence of ARCA modification is unfavorable and seems to be unnecessary.

Other triphosphate dinucleotide analogs that have been successfully used for capping transcripts and for which translation efficiency in the RRL have been measured, are those containing various modifications in the 5′,5′ triphosphate bridge. The best translational properties were obtained for RNAs capped with analogs with a nonbridging sulfur atom in the β-position (so-called β-S-ARCA), which showed a 2–2.5-fold increase of translation efficiency compared to m^7GpppG-capped RNA and those containing dithiophosphates at the α and β positions (Strenkowska et al. 2016). For the latter, the translation efficiency was 1.8–3.2-fold higher than for the m^7GpppG capped RNA, depending on whether it was a stereoisomeric mixture (3.2-fold higher) or a single stereoisomer. In conclusion, it appears that the tested analogs (1–6) which contain only a single modification at the N2 position show very favorable inhibitory properties in the RRL, better even than ARCA compounds with nonbridging sulfur.

The presence of cap analogs attached to mRNA affected translation in HEK293 cells in a different way than in the RRL system. The best result was obtained for mRNA containing (4-Cl-bn)$^2m^7$GpppG (3). This compound was also among the best in the in vitro translation system classification. It is characterized by high affinity for eIF4E and high incorporation efficiency. These features must have contributed to its success. The second score was obtained for compound (4-OCH_3bn)$^2m^7$GpppG (2). This compound ranked in the middle in all measured categories, that together may influence protein synthesis. The third result in translation efficiency in HEK cells was obtained for the (4-(diOCH_3-bn)-tz)$^2m^7$GpppG (4), which incorporates into mRNA almost solely in the correct orientation. This feature must have compensated both weaker affinity for eIF4E and lower efficiency of incorporation than showed by other compounds in the tested group. It is difficult to compare translation efficiency between different cell lines. Previous data demonstrate that the same cap analogs affect the translational potential of different cells in different ways. Our measurements for ARCA counterparts of compounds bn^2m^7GpppG (1), and (4-OCH_3bn)$^2m^7$GpppG (2) in HEK293 cells may provide a reference for this study (Kocmik et al. 2018). Importantly, in these experiments, identical results were obtained for the control $m_2^{7,3'O}$GpppG-mRNA (1.46-fold higher translation relative to m^7GpppG). For compound (2), the same level of translation was noted regardless of whether it had an ARCA-type modification or not. In contrast, a stronger effect on translation efficiency was observed for the bn^2m^7GpppG

(1) counterpart with ARCA modification than for the compound (1) itself. The difference is particularly noticeable when the ARCA modification is located at the 3′-*O* position, and thus at a greater distance from the N2 modification. As we showed, analog (1) is incorporated in the reverse orientation in ~30%, so it is possible that this fraction is the cause of the weakened result.

Additionally, in a cell, many factors have a profound effect on the final outcome. Cells contain sensors in their cytoplasm that respond to the presence of foreign RNA(s). Both the addition of a noncapped transcript and the presence of a fraction with a reverse-inserted analog can easily stimulate the cell response and lead to the inhibition of translation. The literature data point to proteins of the IFIT family, particularly IFIT1, that upon stimulation of the cellular response are abundantly produced and bind foreign-like transcripts. Therefore, the translational potential of mRNAs capped with new analogs is the combination of several parameters and does not directly reflect any of them.

Summing up, the presented N2 modified dinucleotide cap analogs show very favorable biological properties compared to the commonly used m^7GpppG and $m_2^{7,3'O}$GpppG caps. They show a much better ability to inhibit translation in RRL (4.7–15.7 stronger inhibition as compared to the control m^7GpppG). RNAs capped in the IVT reaction with compounds 1–6 show better translational properties, both in the cell-free system of rabbit reticulocytes (1.9–3.4 times higher translation efficiency compared to m^7GpppG, and 1.3–2.3 times compared to $m_2^{7,3'O}$GpppG) and in HEK293 cells (total protein expression was increased 1.4–2.3 times compared to the standard m^7GpppG-RNA and 1.1–1.8 times compared to $m_2^{7,3'O}$GpppG-capped RNA). All compounds were incorporated into RNA preferentially in the correct orientation and (4-(diOCH_3-bn)-tz)$^2m^7$GpppG (4) was incorporated, similar to ARCA-modified RNA, only in the correct orientation. In summary, the dinucleotide cap analogs with substituents at the N2 position exhibit significantly improved properties over the commonly used m^7GpppG and ARCA RNA in capping reactions. In addition, due to their diverse properties, they offer the possibility of selecting an appropriate compound depending on the desired characteristics of the RNA product.

MATERIALS AND METHODS

Synthesis and characterization of new compounds

All used reagents were purchased in the highest available purity from Sigma-Aldrich Chemical Co. (currently Merck) and were used without any further treatment. Triethylammonium bicarbonate (TEAB) buffer was prepared by bubbling CO_2 through an ice-cold aqueous solution of redistilled triethylamine. Intermediate nucleotides were separated by ion-exchange chromatography on a DEAE-Sephadex A-25 (HCO^{3-} form) using a linear gradient of TEAB buffer pH 7.6. Fractions containing products were pooled, evaporated under reduced pressure with several additions of ethanol and isolated as triethylammonium salts. Final cap analogs were separated from reaction mixtures on reversed-phase HPLC columns. Semipreparative HPLC was performed on a Knauer instrument, using the Supelcosil LC-18-DB column (10 × 250 mm, flow rate 3.0 mL min^{-1}) with a linear gradient of methanol from 0 to 50% (v/v) in 0.05 M ammonium acetate (pH 5.9). UV detection was performed at 254 nm. MS spectra were acquired using a Waters Micromass Q-TOF Premier Spectrometer with positive electrospray ionization source. ^{1}H NMR and ^{31}P NMR spectra were recorded on a Varian INOVA 500 MHz spectra. *J* values are given in Hz. N2-[(3-phenylisoxazol-5-yl)methyl]-7-methylguanosine-5′-monophosphate used for the preparation of compound 5 was prepared as previously described in Piecyk et al. (2020a), and compounds 1–4 were prepared as described in Piecyk et al. (2014, 2015).

Synthesis of P^1-N^2-[(3-phenylisoxazol-5-yl)propyl]-7-methylguanosine-5′-P^3-guanosine-5′-triphosphate (5)

To a stirred solution of N2-[(3-phenylisoxazol-5-yl)methyl]-7-methylguanosine-5′-monophosphate (14 mg, 0.019 mmol, TEA salt, prepared as previously described [1]) and imGDP (18 mg, 0.035 mmol) in 0,5 mL of dry DMF, zinc chloride was added (25 mg, 0,18 mmol). The reaction mixture was quenched by addition of aqueous solution of EDTA of (157 mg, 0.42 mmol, disodium salt) after 25 h. The resulting solution was loaded on a DEAE Sephadex column. The desired product was eluted using a linear gradient of 0–0.9M TEAB and the fractions containing the product were pooled, evaporated, and concentrated. The of the product as TEA salt was dissolved in water and then purified by semipreparative RP HPLC (gradient elution 0%–50% MeOH in 0.05 M ammonium acetate buffer pH 5.9) to afford ammonium salt of dinucleotide. Yield: 4.7 mg, 0.007 mmol, 37%. ^{1}H NMR (600 MHz, D_2O) (Supplemental Fig. S1) m7G: δ 9.03 (s, ^{1}H, H8), 7.69 (d, ^{2}H), 7.48–7.43 (m, 3H,Ph), 6.80 (s, ^{1}H, isoxsazole), 5.97 (d, ^{1}H, J = 2.98 Hz, H-1′), 4.74–4.75 (m, ^{2}H, NH-CH_2), 4.53 (t, ^{1}H, J = 3.62 Hz, H-2′), 4.43–4.40 (m, ^{2}H, H-3′, H-4′), 4.26–4.24 (m, ^{2}H, H-5′, H-5″), 4.04 (s, ^{3}H, N7-CH_3); G: δ 7.92 (s, ^{1}H, H8), 5.69 (d, ^{1}H, J = 5.62.Hz, H-1′), 4.59 (t, ^{1}H, J = 5.15 Hz, H-2′), 4.43–4.40 (m, ^{1}H, H-3′), 4.36–4.35 (m, ^{1}H, H-4′), 4.26–4.24 (m, ^{1}H, H-5′), 4.20–4.18 (m, ^{1}H, H-5″); ^{31}P NMR (243 MHz, D_2O, Supplemental Fig. S2): −12.69 (2P, Pα,γ), −23,69 (^{1}P, Pβ); HRMS (ES+) m/z: (M + H)+ (Supplemental Fig. S3): 960.14746, calculated for $C_{31}H_{37}N_{11}O_{19}P_3^+$: 960.14745.

Synthesis of N2-(3-(4-methylthiazol-2-yl)propyl) guanosine (6a)

N2-fluoro-2′,3′,5′-*O*-triacetyl-O^6-(2-(4-nitrophenyl)ethyl)inosine (500 mg, 0.9 mmol) was dissolved in 4 mL of anhydrous dimethylsulfoxide (DMSO), and 3-(4-methylthiazol-2-yl)propyl-1-amine (1.8 mmol) was added. The reaction mixture was stirred at room temperature for 4 h until the 2-fluorine inosine fully reacted. Next, H_2O was added and the reaction mixture was extracted with ethyl acetate several times. The organic layers were concentrated and the resulting oily residue was treated with dimethylamine. The reaction mixture was stirred at 50°C for 2 d. Finally,

dichloromethane (CH_2Cl_2) and diethyl ether were added to induce precipitation of a fine yellow-white powder to obtain N2-(3-(4-methylthiazol-2-yl)propyl)guanosine: 70%, 0.62 mmol, 262 mg; m/z: $(M + H)^+$: 423.0865.

Synthesis of N2-(3-(4-methylthiazol-2-yl)propyl) guanosine-5′-monophosphate (6b)

Phosphorus oxychloride ($POCl_3$) (23 µL, 0.24 mmol) and trimethyl phosphate (82 µL, 0.7 mmol) were added to the N2-(3-(4-methylthiazol-2-yl)propyl)guanosine (30 mg, 0.07 mmol). The reaction mixture was stirred at 0°C for 5 h. Then the solution was neutralized by addition of 1.4 M TEAB and was purified by ion-exchange chromatography on a DEAE-Sephadex A-25 column using a linear 0–1.0 M TEAB gradient. Next the measurement of the absorbance radiation was performed and the fractions containing product were collected and evaporated. The product dissolved in H_2O and was lyophilized obtaining a fine white powder, N2-(3-(4-methylthiazol-2-yl)propyl)guanosine-5′-monophosphate: 40.6%, 0.03 mmol, 14.5 mg; m/z: $(M + H)^+$: 502.9985.

Synthesis of N2-(3-(4-methylthiazol-2-yl)propyl)-7-methylguanosine-5′-monophosphate (6c)

Compound 6b (50 mg, 0.1 mmol) was dissolved in 0.55 mL anhydrous dimethylsulfoxide and methyl iodide (61 µL, 0.1 mmol) was added. The reaction mixture was stirred at room temperature for 3.5 h. Then water (6 mL) was added and the solution was extracted four times with diethyl ether (4 × 8 mL). The aqueous phases were purified on DEAE-Sephadex A-25 using a linear gradient 0–1.0 M of TEAB. Product was lyophilized to yield N2-(3-(4-methylthiazol-2-yl)propyl)-7-methylguanosine-5′-monophosphate: 11.2%, 0.011 mmol, 5.7 mg; m/z: $(M + H)^+$: 517.0535.

Synthesis of N2-(3-(4-methylthiazol-2-yl)propyl)-7-methylguanosine-5′-P^3-guanosine-5′-triphosphate (6)

Guanosine 5′-diphosphate imidazolide (25 mg, 0.05 mmol) and $ZnCl_2$ (33 mg, 0.24 mmol) were stirred in anhydrous DMF (0.7 mL) with N2-(3-(4-methylthiazol-2-yl)propyl)-7-methylguanosine-5′-monophosphate (31 mg, 0.06 mmol) at room temperature for 24 h. The reaction mixture was poured into a solution of EDTA (114 mg, 0.3 mmol) in water (1.5 mL) and neutralized to pH 7 by addition of 1 M TEAB. The product was separated from the reaction mixture by chromatography on a DEAE–Sephadex using a 0–1.0 M gradient of TEAB. Product was obtained as colorless crystals. The final dinucleotide cap analog was additionally purified on a reversed-phase HPLC column to yield (6): 6 mg (0.063 mmol), 48%, ammonium salt; ^{1}H NMR (600 MHz, D_2O) (Supplemental Fig. S4) m7G: δ 9.01 (s, ^{1}H, H_8), 7.00 (s,^{1}H, thiazole), 5.92 (d, ^{1}H, J = 3.12 Hz, H-1′), 4.57 (t, ^{1}H, J = 4.73 Hz, H-2′), 4,47–4,42 (m, ^{2}H, H-3′, H-4′), 4.33–4.31 (m, ^{1}H, H-5′), 4.29–4.21 (m, ^{1}H, H-5′), 4.06 (s, ^{3}H, N7-CH_3), 3.54–3.46 (m, ^{2}H, NCH_2), 3.10 (t, ^{2}H, CH_2-*CH_2*-CH_2), 2.31 (s, ^{3}H, CH_3 thiazole), 2.15–2.11 (m, ^{2}H, CH_2-CH_2-*CH_2*); G: δ 8.01 (s, ^{1}H, H_8), 5.78 (d, ^{1}H, J = 5.93 Hz, H-1′), 4.63 (t, ^{1}H, J = 5.19 Hz, H-2′), 4.47–4.42 (m, ^{1}H, H-3′), 4.40–4.38 (m, ^{1}H, H-4′), 4.29–4.21 (m, ^{2}H, H-5′, H-5′). ^{31}P NMR (243 MHz, D_2O, Supplemental Fig. S5): −11.95 (2P, Pα,γ), −23.47 (^{1}P, Pβ); HRMS (ES+) m/z: $(M + H)^+$ (Supplemental Fig. S6): 943.14677, calculated for $C_{28}H_{39}N_{11}O_{18}P_3S^+$: 943.14808.

Synthesis of luciferase encoding mRNAs

PCR product containing the firefly luciferase coding sequence and SP6 promoter sequence, purified with the NucleoSpin Gel and PCR Clean-up (Macherey Nagel) was used as a dsDNA template for IVT. RNA capping was carried out cotranscriptionally using the newly synthesized analogs (molar ratio of cap:GTP was 5:1). As described previously, the transcription reaction contained: transcription buffer, 25 ng/µL of dsDNA template, 0.5 mM ATP/CTP/UTP, 0.1 mM GTP, 0.5 mM dinucleotide cap analog, 0.5 U/µL of Ribolock Ribonuclease Inhibitor, and 1 U/µL of SP6 RNA polymerase (Thermo Fisher Scientific) (Strenkowska et al. 2016). The IVT reaction mixture was incubated for 1 h at 37°C, then 0.025 U/µL of DNase I (Thermo Scientific) was added and incubated with the IVT reaction mixture for 20 min at 37°C to remove template DNA. The reaction mixture was purified using the NucleoSpin RNA Clean-Up (Macherey-Nagel) according to the manufacturer's instructions. The integrity of transcripts was checked on a nondenaturing 1% agarose gel and concentration was determined spectrophotometrically.

Translation measurement in RRL system

The expression level of luciferase-encoding mRNAs capped with newly synthesized cap analogs was measured in Flexi RRL system (Rabbit Reticulocyte Lysate, Promega) as described previously (Strenkowska et al. 2016). Each tube contained 10 µL of reaction mixture consisting of 40% Flexi RRL lysate, 0.01 mM amino acid mix, 0.9 mM magnesium acetate (1.8 mM endogenous lysate magnesium concentration) and 190 mM potassium acetate. Samples were preincubated for 60 min at 30°C before mRNA addition. The translation reaction was carried out under the same conditions for additional 60 min. The activity of synthesized luciferase was measured using a GloMax luminometer.

Cell culture

HEK293 cells were cultured in Dulbecco's modified Eagle's medium (DMEM, Biowest) supplemented with 10% fetal bovine serum (Biowest) and penicillin-streptomycin solution (Biowest) at 37°C in a humidified atmosphere of 5% CO_2.

mRNA transfection

Twenty-four hours before the transfection, HEK293 cells were seeded at a density of 3×10^4 per well on 96-well plates, pretreated with poli-L-lysine (1 h incubation with 100 µg mL PLL). The culture medium was changed to fresh (without antibiotics) just before the transfection, which was carried out with TransiT-mRNA (Mirus Bio LLC) according to the manufacturer's procedure. Briefly, 100 ng of analog-capped mRNA mixed with the transfectant and OptiMEM was incubated for 10–30 min prior to transfection of 3×10^4 cells. Cells treated with the transfection mix without mRNA served as a negative control in the experiment. Four hours

post-transfection the culture medium was changed to fresh with antibiotics. The cells were incubated at 37°C in a humidified atmosphere of 5% CO_2 and harvested 4, 12, 24, and 48 h post-transfection.

Luciferase reporter assays

HEK293 cells transfected with analog-capped mRNAs were lysed by addition of 20 µL per well of Cell Culture Lysis Reagent (Promega). To estimate the luciferase activity, the lysate was mixed with the luciferase substrate (Promega) in a ratio of 1:4, and the luminescence was measured on a Synergy H1MFDG Microplate Reader (BioTek). To avoid errors due to varying numbers of cells in each well, the total protein concentration of the lysates was determined with Roti-Quant Protein quantitation assay according to Bradford (Roth) using BSA as standard. The luminescence was normalized to the protein concentration and translation level was calculated as the percent of the luciferase activity of m^7GpppG-capped mRNA.

Translational inhibition

The inhibitory potential of the new cap analogs was measured in RRL reaction mix (Flexi Rabbit Reticulocyte Lysate, Promega) in a volume of 12.5 µL and under conditions determined for cap-dependent translation as previously described (Kowalska et al. 2009). Briefly, reaction mixture was first preincubated for 60 min at 30°C and then a mixture of $m_2^{7,3'O}$GpppG-capped mRNA encoding the luciferase reporter protein and the cap analog to be tested was added. The samples were incubated for an additional 60 min at 30°C. Luciferase activity was measured instantaneously using a GloMax luminometer (Promega). IC_{50} values were determined by nonlinear regression analysis of the experimental data using GraphPad Prism 6. IC_{50} values are mean ± SD from at least three independent replicates.

Thermal stability assay

Thermal stability of murine eIF4E (28–217 aa) was analyzed by differential scanning fluorimetry (DSF), as described previously (Piecyk et al. 2020b). Briefly, the assay sample (25 µL) contained 5× SYPRO Orange (Sigma-Aldrich) and 4 µM of eIF4E (final concentration), in HEPES/KOH with 100 mM KCl, 0.5 mM EDTA, and 1 mM DTT (pH 7.2). Tested compounds were added at 100 µM final concentration (single point experiments), or in the range from 1 µM to 100 µM. A CFX96 Real-Time PCR (Bio-Rad) was used to increase the temperature starting from 22°C to 95°C, with the temperature ramp 0.5°C/30 sec, and fluorescence intensity (FRET channel) was measured at each step. The melting temperature (T_m) was then calculated using CDpal software (Niklasson et al. 2015).

In vitro synthesis of short analog-capped 25-nt mRNAs

A duplex DNA sequence containing the sequence of SP6 promoter (underlined) was prepared by annealing of two complementary primers: 5′ATACGATTTAGGTGACACTATAGAAGAAGCGGGCATGCGGCCAGCCATAGCCGATCA3′ and 5′TGATCGGCTATGGCTGGCCGCATGCCCGCTTCTTCTATAGTGTCACCTAAATCGTAT3′. Annealing reaction was conducted in 10 mM Tris pH 7.4, 1 mM $MgCl_2$, 100 mM NaCl, and 25 µM primers for 2′ at 95°C in water bath, subsequently cooled down to 30°C–35°C for 1 h and then quickly to 25°C. Thus, the prepared template was used for the IVT reaction with cotranscriptional capping (cap: GTP ratio 10: 1). The reaction was conducted overnight at 37°C in 20 µL containing: 200× diluted template DNA, transcription buffer, 0.5 mM ATP/CTP/UTP, 0.125 mM GTP, 1.25 mM cap analog, 0.5 U/µL of Ribolock Ribonuclease Inhibitor and 1 U/µL of SP6 RNA polymerase (Thermo Fisher Scientific). Template DNA was then digested with DNase I (Thermo Fisher Scientific) in 30′ incubation at 37°C, and the 35-nt product was purified using an Oligo Clean-Up and Concentration kit (Norgen Biotek) according to the manufacturer's instructions. To specifically cleave off the heterogenous 3′ ends of the transcripts, mRNA was treated with DNazyme 5′TGATCGGCTAGGCTAGCTACAACGAGGCTGGCCGC3′. Reaction mixture containing 30 pmoles of DNazyme per 400 ng RNA in 50 mM Tris pH 7.4 and 50 mM $MgCl_2$ was incubated for 1 h at 37°C. DNazyme was then digested with DNase I (Thermo Fisher Scientific) in 30′ incubation at 37°C, and the homogenous 3′ end 25-nt transcripts capped with the appropriate cap analog (1–7) were purified using an Oligo Clean-Up and Concentration kit (Norgen Biotek) according to the manufacturer's instructions.

Decapping with hNudt 16 and hDcp2

To investigate the susceptibility of dinucleotide cap analogs to hydrolysis with hNudt16 and hDcp2, a 50 ng analog-capped 25-nt RNA was used. The reaction mixture (7 µL) of 40 mM Tris pH 7.9, 100 mM NaCl, 6 mM $MgCl_2$, 2 mM DTT, and 2.5 µM hNudt16 was subjected to 30 min incubation at 37°C and stopped by addition of 2× RNA loading dye (95% formamide, 0.025% SDS, 0.025% bromophenol blue, 0.025% xylene cyanol FF, 0.025% ethidium bromide, 0.5 mM EDTA) followed by 5 min incubation at 75°C. For cap hydrolysis with hDcp2, the reaction mixture (7 µL) contained 10 mM HEPES pH 7.5, 100 mM KOAc, 2 mM MgOAc, 0.5 mM $MnCl_2$, 2 mM DTT, and 1.4 µM hDcp2. Reaction was conducted as described for hNudt16. Samples were separated on an RNA sequencing gel (15% polyacrylamide/7 M urea), stained with SYBR Gold (Life Technologies) and visualized using a UV-transilluminator (ChemiDoc MP Imaging System, Bio-Rad). Densitometric analysis using Image Lab software (Bio-Rad) was used to determine the level of cap hydrolysis. Decapping was calculated as the percent loss in the capped band after addition of the enzyme. The data represent the mean ± SD from three experiments.

SUPPLEMENTAL MATERIAL

Supplemental material is available for this article.

ACKNOWLEDGMENTS

We thank Dr. Anna Niedzwiecka for providing the murine eIF4E (28-217aa) protein and Mr. Michal Tyras for the Dcp2 protein.

Financial support for this work was provided by the National Science Centre, Poland, grant nos. UMO/2018/31/B/ST5/03544 (M.J.A.), UMO-2019/33/B/NZ1/01322 (E.D.), UMO/2017/27/B/NZ1/01859 (E.D.), and UMO/2016/21/D/ST501654 (K.P.).

Author contributions: K.P., K.K., and M.J.A. synthesized new compounds. R.G., A.S.D., P.P., and M.L. performed the experiments. R.G. produced the Nudt16 protein. R.G., K.P., E.D., and M.J.A. analyzed the data and wrote the paper.

Received September 22, 2022; accepted November 3, 2022.

REFERENCES

Baden LR, El Sahly HM, Essink B, Kotloff K, Frey S, Novak R, Diemert D, Spector SA, Rouphael N, Creech CB, et al. 2021. Efficacy and safety of the mRNA-1273 SARS-CoV-2 vaccine. *N Engl J Med* **384:** 403–416. doi:10.1056/NEJMoa2035389

Cai A, Jankowska-Anyszka M, Centers A, Chlebicka L, Stepinski J, Stolarski R, Darzynkiewicz E, Rhoads RE. 1999. Quantitative assessment of mRNA cap analogues as inhibitors of in vitro translation. *Biochemistry* **38:** 8538–8547. doi:10.1021/bi9830213

Chrabąszczewska M, Winiewska-Szajewska M, Ostrowska N, Bojarska E, Stępiński J, Mancewicz Ł, Łukaszewicz M, Trylska J, Taube M, Kozak M, et al. 2021. Insight into the binding and hydrolytic preferences of hNudt16 based on nucleotide diphosphate substrates. *Int J Mol Sci* **22:** 10929. doi:10.3390/ijms222010929

Furuichi Y. 2015. Discovery of m^7G-cap in eukaryotic mRNAs. *Proc Jpn Acad Ser B Phys Biol Sci* **91:** 394–409. doi:10.2183/pjab.91.394

Galloway A, Cowling VH. 2019. mRNA cap regulation in mammalian cell function and fate. *Biochim Biophys acta Gene Regul Mech* **1862:** 270–279. doi:10.1016/j.bbagrm.2018.09.011

Grudzien-Nogalska E, Stepinski J, Jemielity J, Zuberek J, Stolarski R, Rhoads RE, Darzynkiewicz E. 2007. Synthesis of anti-reverse cap analogs (ARCAs) and their applications in mRNA translation and stability. *Methods Enzymol* **431:** 203–227. doi:10.1016/S0076-6879(07)31011-2

Grzela R, Nasilowska K, Lukaszewicz M, Tyras M, Stepinski J, Jankowska-Anyszka M, Bojarska E, Darzynkiewicz E. 2018. Hydrolytic activity of human Nudt16 enzyme on dinucleotide cap analogs and short capped oligonucleotides. *RNA* **24:** 633–642. doi:10.1261/rna.065698.118

Jemielity J, Fowler T, Zuberek J, Stepinski J, Lewdorowicz M, Niedzwiecka A, Stolarski R, Darzynkiewicz E, Rhoads RE. 2003. Novel "anti-reverse" cap analogs with superior translational properties. *RNA* **9:** 1108–1122. doi:10.1261/rna.5430403

Kadokura M, Wada T, Urashima C, Sekine M. 1997. Efficient synthesis of γ-methyl-capped guanosine 5′-triphosphate as a 5′-terminal unique structure of U6 RNA via a new triphosphate bond formation involving activation of methyl phosphorimidazolidate using ZnCl2 as a catalyst in DMF under anhydrous conditions. *Tetrahedron Lett* **38:** 8359–8362. doi:10.1016/S0040-4039(97)10263-5

Kalek M, Jemielity J, Grudzien E, Zuberek J, Bojarska E, Cohen LS, Stepinski J, Stolarski R, Davis RE, Rhoads RE, et al. 2011. Synthesis and biochemical properties of novel mRNA 5′ cap analogs resistant to enzymatic hydrolysis. *Nucleosides Nucleotides Nucleic Acids* **24:** 615–621. doi:101081/NCN-200060091

Kocmik I, Piecyk K, Rudzinska M, Niedzwiecka A, Darzynkiewicz E, Grzela R, Jankowska-Anyszka M. 2018. Modified ARCA analogs providing enhanced translational properties of capped mRNAs. *Cell Cycle* **17:** 1624–1636. doi:10.1080/15384101.2018.1486164

Kowalska J, Lewdorowicz M, Zuberek J, Grudzien-Nogalska E, Bojarska E, Stepinski J, Rhoads RE, Darzynkiewicz E, Davis RE, Jemielity J. 2008. Synthesis and characterization of mRNA cap analogs containing phosphorothioate substitutions that bind tightly to eIF4E and are resistant to the decapping pyrophosphatase DcpS. *RNA* **14:** 1119–1131. doi:10.1261/rna.990208

Kowalska J, Lukaszewicz M, Zuberek J, Ziemniak M, Darzynkiewicz E, Jemielity J. 2009. Phosphorothioate analogs of m^7GTP are enzymatically stable inhibitors of cap-dependent translation. *Bioorg Med Chem Lett* **19:** 1921–1925. doi:10.1016/j.bmcl.2009.02.053

Kowalska J, Del Nogal AW, Darzynkiewicz ZM, Buck J, Nicola C, Kuhn AN, Lukaszewicz M, Zuberek J, Strenkowska M, Ziemniak M, et al. 2014. Synthesis, properties, and biological activity of boranophosphate analogs of the mRNA cap: versatile tools for manipulation of therapeutically relevant cap-dependent processes. *Nucleic Acids Res* **42:** 10245–10264. doi:10.1093/nar/gku757

Miedziak B, Dobiezynska A, Darzynkiewicz ZM, Bartkowska J, Miszkiewicz J, Kowalska J, Warminski M, Tyras M, Trylska J, Jemielity J, et al. 2019. Kinetic analysis of IFIT1 and IFIT5 interaction with different native and engineered RNAs and its consequences for designing mRNA-based therapeutics. *RNA* **26:** 58–68. doi:10.1261/rna.073304.119

Milligan JF, Groebe DR, Witherell GW, Uhlenbeck OC. 1987. Oligoribonucleotide synthesis using T7 RNA polymerase and synthetic DNA templates. *Nucleic Acids Res* **15:** 8783–8798. doi:10.1093/nar/15.21.8783

Niedzwiecka A, Marcotrigiano J, Stepinski J, Jankowska-Anyszka M, Wyslouch-Cieszynska A, Dadlez M, Gingras AC, Mak P, Darzynkiewicz E, Sonenberg N, et al. 2002. Biophysical studies of eIF4E cap-binding protein: recognition of mRNA 5′ cap structure and synthetic fragments of eIF4G and 4E-BP1 proteins. *J Mol Biol* **319:** 615–635. doi:10.1016/S0022-2836(02)00328-5

Niesen FH, Berglund H, Vedadi M. 2007. The use of differential scanning fluorimetry to detect ligand interactions that promote protein stability. *Nat Protoc* **2:** 2212–2221. doi:10.1038/nprot.2007.321

Niklasson M, Andresen C, Helander S, Roth MGL, Zimdahl Kahlin A, Lindqvist Appell M, Lundström P. 2015. Robust and convenient analysis of protein thermal and chemical stability. *Protein Sci* **24:** 2055–2062. doi:10.1002/pro.2809

Pasquinelli AE, Dahlberg JE, Lund E. 1995. Reverse 5′ caps in RNAs made in vitro by phage RNA polymerases. *RNA* **1:** 957–967.

Peng ZH, Sharma V, Singleton SF, Gershon PD. 2002. Synthesis and application of a chain-terminating dinucleotide mRNA cap analog. *Org Lett* **4:** 161–164. doi:10.1021/ol0167715

Piecyk K, Lukaszewicz M, Darzynkiewicz E, Jankowska-Anyszka M. 2014. Triazole-containing monophosphate mRNA cap analogs as effective translation inhibitors. *RNA* **20:** 1539–1547. doi:10.1261/rna.046193.114

Piecyk K, Niedzwiecka A, Ferenc-Mrozek A, Lukaszewicz M, Darzynkiewicz E, Jankowska-Anyszka M. 2015. How to find the optimal partner–studies of snurportin 1 interactions with U snRNA 5′ TMG-cap analogues containing modified 2-amino group of 7-methylguanosine. *Bioorg Med Chem* **23:** 4660–4668. doi:10.1016/j.bmc.2015.05.054

Piecyk K, Lukaszewicz M, Kamel K, Janowska M, Pietrow P, Kmiecik S, Jankowska-Anyszka M. 2020a. Isoxazole-containing 5′ mRNA cap analogues as inhibitors of the translation initiation process. *Bioorg Chem* **96:** 103583. doi:10.1016/j.bioorg.2020.103583

Piecyk K, Pietrow P, Arnold T, Worch R, Korneeva NL, Jankowska-Anyszka M. 2020b. Effect of HIV-1 TAT peptide fusion on 5′ mRNA cap analogs cell membrane permeability and translation inhibition. *Bioconjug Chem* **31:** 1156–1166. doi:10.1021/acs.bioconjchem.0c00080

Polack FP, Thomas SJ, Kitchin N, Absalon J, Gurtman A, Lockhart S, Perez JL, Pérez Marc G, Moreira ED, Zerbini C, et al. 2020.

Safety and efficacy of the BNT162b2 mRNA Covid-19 vaccine. *N Engl J Med* **383:** 2603–2615. doi:10.1056/NEJMoa2034577

Raper SE, Chirmule N, Lee FS, Wivel NA, Bagg A, Gao GP, Wilson JM, Batshaw ML. 2003. Fatal systemic inflammatory response syndrome in a ornithine transcarbamylase deficient patient following adenoviral gene transfer. *Mol Genet* **80:** 148–158. doi:10.1016/j.ymgme.2003.08.016

Rydzik AM, Kulis M, Lukaszewicz M, Kowalska J, Zuberek J, Darzynkiewicz ZM, Darzynkiewicz E, Jemielity J. 2012. Synthesis and properties of mRNA cap analogs containing imidodiphosphate moiety—fairly mimicking natural cap structure, yet resistant to enzymatic hydrolysis. *Bioorg Med Chem* **20:** 1699–1710. doi:10.1016/j.bmc.2012.01.013

Sahin U, Kariko K, Tureci O. 2014. mRNA-based therapeutics—developing a new class of drugs. *Nat Rev Drug Discov* **13:** 759–780. doi:10.1038/nrd4278

Sahin U, Muik A, Derhovanessian E, Vogler I, Kranz LM, Vormehr M, Baum A, Pascal K, Quandt J, Maurus D, et al. 2020. COVID-19 vaccine BNT162b1 elicits human antibody and T_H1 T cell responses. *Nature* **586:** 594–599. doi:10.1038/s41586-020-2814-7

Sousa R, Padilla R. 1995. A mutant T7 RNA polymerase as a DNA polymerase. *EMBO J* **14:** 4609–4621. doi:10.1002/j.1460-2075.1995.tb00140.x

Stepinski J, Waddell C, Stolarski R, Darzynkiewicz E, Rhoads RE. 2001. Synthesis and properties of mRNAs containing the novel "anti-reverse" cap analogs 7-methyl(3′-*O*-methyl)GpppG and 7-methyl (3′-deoxy)GpppG. *RNA* **7:** 1486–1495.

Strenkowska M, Grzela R, Majewski M, Wnek K, Kowalska J, Lukaszewicz M, Zuberek J, Darzynkiewicz E, Kuhn AN, Sahin U, et al. 2016. Cap analogs modified with 1,2-dithiodiphosphate moiety protect mRNA from decapping and enhance its translational potential. *Nucleic Acids Res* **44:** 9578–9590. doi:10.1093/nar/gkw896

Suydam IT, Strobel SA. 2009. Nucleotide analog interference mapping. *Methods Enzymol* **468:** 3–30. doi:10.1016/S0076-6879(09)68001-0

Vivoli M, Novak HR, Littlechild JA, Harmer NJ. 2014. Determination of protein-ligand interactions using differential scanning fluorimetry. *J Vis Exp* 51809. doi:10.3791/51809

Vlatkovic I, Ludwig J, Boros G, Szabó GT, Reichert J, Buff M, Baiersdörfer M, Reinholz J, Mahiny AJ, Şahin U, et al. 2022. Ribozyme assays to quantify the capping efficiency of *in vitro*-transcribed mRNA. *Pharmaceutics* **14:** 328. doi:10.3390/pharmaceutics14020328

Volpon L, Osborne MJ, Topisirovic I, Siddiqui N, Borden KLB. 2006. Cap-free structure of eIF4E suggests a basis for conformational regulation by its ligands. *EMBO J* **25:** 5138–5149. doi:10.1038/sj.emboj.7601380

Weissman D. 2015. mRNA transcript therapy. *Expert Rev Vaccines* **14:** 265–281. doi:10.1586/14760584.2015.973859

Wojcik R, Baranowski MR, Markiewicz L, Kubacka D, Bednarczyk M, Baran N, Wojtczak A, Sikorski PJ, Zuberek J, Kowalska J, et al. 2021. Novel N7-arylmethyl substituted dinucleotide mRNA 5′ cap analogs: synthesis and evaluation as modulators of translation. *Pharmaceutics* **13:** 1941. doi:10.3390/pharmaceutics13111941

Ziemniak M, Strenkowska M, Kowalska J, Jemielity J. 2013. Potential therapeutic applications of RNA cap analogs. *Future Med Chem* **5:** 1141–1172. doi:10.4155/fmc.13.96

MEET THE FIRST AUTHOR

Renata Grzela

***Meet the First Author(s)* is an editorial feature within *RNA*, in which the first author(s) of research-based papers in each issue have the opportunity to introduce themselves and their work to readers of *RNA* and the RNA research community. Renata Grzela is the first author of this paper, "N2 modified dinucleotide cap analogs as a potent tool for mRNA engineering." Renata is an Assistant Professor in the Division of Biophysics of the Institute of Experimental Physics at the University of Warsaw. Her research focuses on mRNA degradation, immunogenicity of mRNA, and the applications of mRNA.**

What are the major results described in your paper and how do they impact this branch of the field?

In this paper, we presented the synthesis and characterization of new compounds that can be widely used in biotechnology and medicine to prepare improved RNA molecules. mRNA-based drugs are a rapidly growing branch of new innovative therapeutics. Our patented compounds present extremely appealing alternatives to those currently on the market.

What led you to study RNA or this aspect of RNA science?

Although we have a plethora of drugs on the pharmaceutical market, we are still unable to provide treatment strategies for many diseases. Sometimes this is because research is too expensive and, as in the case of rare diseases, unprofitable. And other times, it is due to obstacles in delivering effective molecules. On the other hand, we have therapies that are fraught with severe side effects, such as chemotherapy. mRNA is an amazing molecule since drugs based on it can be produced quickly and cost-effectively. Furthermore, mRNA therapy has no harmful effects on the patient and is usually associated with no or mild side effects. These features of RNA prompted me to devote my time and effort to the development of modern mRNA-based drugs.

Continued

During the course of these experiments, were there any surprising results or particular difficulties that altered your thinking and subsequent focus?

It was extremely interesting to discover that modification of guanine at the N2 position not only affects its interaction with proteins that recruit the transcript to the biosynthetic apparatus in the cell. It also allows for the correct orientation of dinucleotide incorporation into the mRNA chain. Previously, achieving both features required the introduction of two different modifications and greatly complicated the chemical synthesis of the compounds.

What are some of the landmark moments that provoked your interest in science or your development as a scientist?

The turning points in my development as a scientist were the postdoctoral fellowships. They changed the way I think and plan my research. A particularly difficult moment is the transformation from a doctoral student to an independent scientist. It involves taking responsibility for one's decisions in a much broader way than in the early stages of one's scientific career.

If you were able to give one piece of advice to your younger self, what would that be?

Discuss with other scientists and investigate the scientific problem from different points of view.

Are there specific individuals or groups who have influenced your philosophy or approach to science?

About 10 years ago, I got to know the scientific community working on therapeutic mRNA. I was hugely impressed by Professor Ugur Sahin and Professor Özlem Türeci, two scientists who are visionaries in the field. An extremely inspiring person for me was Professor Katalin Karikó, who, despite many adversities, realized the goal she believed in. Of course, I have to say a word about the Polish community, which is a strong point on the world map of therapeutic mRNA research. It was a pleasure to work with such authorities as Professor Edward Darżynkiewicz and Professor Marzena Jankowska-Anyszka.

What are your subsequent near- or long-term career plans?

I firmly believe that the future will belong to the mRNA molecule. Therefore, I intend to devote the next years of my scientific work to improving mRNA-based drugs. There is still much left to explore and many new therapeutic strategies to propose.